

Diapiric ascent of magmas through power law crust and mantle

Roberto Ferrez Weinberg¹ and Yuri Podladchikov²

The Hans Ramberg Tectonic Laboratory, Institute of Earth Sciences,
Uppsala University, Uppsala, Sweden

Abstract. There has never been a convincing explanation of the way in which diapirs of molten granite can effectively rise through mantle and crust. We argue here that this is mainly because the country rocks have previously been assumed to be Newtonian, and we show that granitoid diapirs rising through thermally graded power law crust may indeed rise to shallow crustal levels while still molten. The ascent velocity of diapirs is calculated through an equation with the form of the Hadamard-Rybczynski equation for the rise of spheres through Newtonian ambient fluids. This well-known equation is corrected by factors dependent on the power law exponent n of the ambient fluid and the viscosity contrast between the drop and the ambient fluid. These correction factors were derived from results reported in the fluid mechanical and chemical engineering literature for the ascent of Newtonian drops through power law fluids. The equation allows calculation of the ascent rates of diapirs by direct application of rheological parameters of rocks. The velocity equation is numerically integrated for the ascent of diapirs through a lithosphere in which the temperature increases with depth. The depth of solidification of the diapir is systematically studied as a function of the geothermal gradient, buoyancy of the body, solidus temperature of the magma, and rheological parameters of the wall rock. The results show that when the wall rock behaves as a power law fluid, the diapir's ascent rate increases, without a similar increase in the rate of heat loss. In this way, diapirs rising at 10 to 10² m/yr can ascend into the middle or upper crust before solidification. Strain rate softening rather than thermal softening is the mechanism that allows diapirism to occur at such rates. The thermal energy of the diapir is used to soften the country rock only at late stages of ascent. The transport of magmas through the lower crust and mantle as diapirs is shown to be as effective as magmatic ascent through fractures.

Introduction

Silicic volcanism demonstrates that granite magmas commonly reach shallow crustal levels. Many authors challenge diapirism as a feasible ascent mechanism because it has never been convincingly demonstrated that magmatic diapirs can reach the shallow crust in geologically reasonable times [e.g., *Paterson et al.*, 1991; *Clemens and Mawer*, 1992]. The ascent of a diapir may be closely approximated by the slow translation (negligible inertia) of a viscous drop through a viscous fluid [e.g., *Marsh*, 1982; *Schmeling et al.*, 1988; *Cruden*, 1988, 1990; *Weinberg*, 1992]. The flow of an infinite Newtonian fluid past a sphere (Stokes flow; Figure 1) is a well-documented problem in fluid dynamics [e.g., *Batchelor*, 1967], and therefore most studies dealing with the ascent of diapirs simplify the wall rock to a Newtonian fluid and disregard the effects of temperature [*Biot and Odé*, 1965; *Whitehead and Luther*, 1975; *Marsh*, 1979; *Marsh and Kantha*, 1978; *Ramberg*, 1981; *Schmeling et al.*, 1988; *Cruden*, 1988,

1990; *Kerr and Lister*, 1988; *Rönnlund*, 1989; *Lister and Kerr*, 1989; *Polyakov and Podladchikov*, 1990; *Weinberg*, 1992].

Several workers have used the structures around granitoid plutons to conclude that the viscosity of the plutons must have been sufficiently similar to their wall rocks during their Stokes-like ascent and that the granitoids must have been highly crystallized [*Berger and Pitcher*, 1970; *Ramberg*, 1970; *Soula*, 1982; *Bateman*, 1984]. Another group of workers follow *Grout* [1932] and suggest that deformation of Newtonian wall rock is confined to narrow aureoles which are thermally softened by heat from the diapir (hot-Stokes models [*Marsh*, 1982; *Morris*, 1982; *Ribe*, 1983; *Daly and Raefsky*, 1985; *Mahon et al.*, 1988]). According to calculations by *Marsh* [1982] a sphere 3 km in radius would be able to rise only halfway through a Newtonian lithosphere before solidifying. Subsequent bodies following the same path, while it is still warm, could reach higher levels. The effect on diapiric ascent of increasing viscosity of the ambient fluid has been studied recently by *Kukowski and Neugebauer* [1990].

However, it is well known from laboratory experiments that at natural strain rates, pressures, and temperatures, mantle and crustal rocks are likely to behave as power law fluids according to

$$\dot{\epsilon} = A e^{-E/RT} \sigma^n \text{ for uniaxial stress} \quad (1)$$

(see notation list and *Kirby* [1983], *Paterson* [1987], and *Wilks and Carter* [1990, and references therein]). When $n =$

¹Now at Research School of Earth Sciences, Australian National University, Canberra.

²Permanently at Institute of Experimental Mineralogy, Russian Academy of Sciences, Chernogolovka.

Copyright 1994 by the American Geophysical Union.

Paper number 93JB03461
0148-0227/94/93JB03461\$05.00

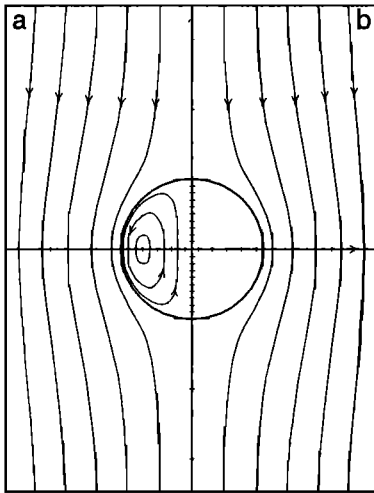


Figure 1. Streamlines in and around a sphere translating through Newtonian fluid (a) viscous sphere (b) solid sphere (Stokes case; redrawn from *Schmeling et al.* [1988]). The streamlines shown will concentrate towards a sphere translating through power law fluids.

1, strain rate varies linearly with stress, the constant viscosity is independent of the strain rate, and the fluid is said to be Newtonian. When n is larger than 1, as in most rocks, the relationship between strain rate and stress is nonlinear, and the effective viscosity of the material decreases with increasing strain rates or stress. Although extrapolating the results of laboratory experiments on rock rheology to geological systems is difficult (see the thorough discussion by *Paterson* [1987]), rock rheology determined by these studies probably better approximates the actual behavior than does the simplification to Newtonian behavior.

Some recent studies try to assess the effects of powerlaw wall rocks on diapiric rise rate [*Morris*, 1982; *Mahon et al.*, 1988; *Miller et al.*, 1988; *England*, 1992]. *Mahon et al.* [1988] found low ascent velocities for diapirs rising through wall rock of olivine rheology at crustal temperatures. *Miller et al.* [1988] use the rheology of Westerly granite to calculate the ascent rate of diapirs and to estimate the strain rates, with which they determine the effective viscosity of the wall rock, on the calculations by *Mahon et al.* [1988]. The influence of power law behavior of the wall rock on diapirism has been hindered by the absence in the literature of a simple equation for the rise of a Newtonian drop through power law fluids. Another hindrance is the lack of a rule for the definition of effective viscosity of media with strong spatial variation in strain rate.

This paper presents an equation for the final velocity of viscous buoyant drops rising through power law ambient fluids. This equation is then applied to the problem of magmatic diapirs rising through the lithosphere. We start by reviewing the fluid mechanical and chemical engineering literature on the rise of drops through power law fluids and rewriting those solutions in the form of the well-known Hadamard-Rybczynski equation (2). We then extrapolate the known solutions to higher values of n that are of interest in geology, and we show how the rheological parameters of rocks can be used in the equation.

The equations controlling diapiric ascent are integrated numerically to calculate the depth and time of solidification of magmatic diapirs rising through lithosphere with defined geothermal gradients. Several parameters are found to control the ascent. The diapir's velocity, temperature, viscosity, and Peclet and Nusselt numbers are calculated, together with the effective viscosity of the surrounding medium and the thickness of the diapir's thermal boundary layer. The calculations take account of the effects of thermal softening of the wall rock by including the drag correction derived by *Daly and Raefsky* [1985]. We illustrate the approach by applying our equations to two examples: (1) a diapir with the well-constrained characteristics of the Tara granodiorite in Australia, ascending through a crust with the properties of Westerly granite [*Miller et al.*, 1988], and (2) the rise of a 10-km radius mantle diapir from a subducting slab 100 km deep. This diapir rises to the base of a 40-km-thick crust where it triggers the formation of a crustal diapir that ascends through a layered crust.

The results indicate that magmatic diapirs may rise through the mantle or lower crust one order of magnitude faster than predicted by earlier studies. In effect, diapirism through power law surroundings can account for magmas reaching shallow crustal levels. In contrast to previous results, we show here that diapirs can rise from the Moho to shallow crust in time spans of only 10^4 to 10^5 years. Alternatively, melts can rise diapirically from the melting zone of subducting plates to high crustal levels in 10^5 to 10^6 years. This approximates the delay between the initiation of subduction and the start of arc volcanicity [*Marsh*, 1982].

Previous Studies

The slow translation of spheres through fluids has been thoroughly studied. *Hadamard* [1911] and *Rybczynski* [1911] extended to viscous spherical drops, Stoke's equation for the velocity of a solid sphere falling through an infinite Newtonian fluid:

$$V = \frac{1}{3} \frac{\Delta \rho g r^2}{\mu} \left(\frac{\mu + \mu_{sph}}{\mu + \frac{3}{2} \mu_{sph}} \right) \quad (2)$$

(see notation list for symbols). Subsequent works have treated the translation of spheres through fluids of other rheologies. Rather than the simple uniaxial stress in (1), the main interest here is the translation of spheres through power law fluids which, for two- or three-dimensional stresses, must be described by the more general equation [*Turcotte and Schubert*, 1982; *Wilks and Carter*, 1990]

$$\sigma_{ij} = K \dot{\gamma}^{m-1} \dot{\epsilon} \quad (3)$$

where $m=1/n$, and $\dot{\gamma}$ is the second invariant of the strain rate tensor $\dot{\epsilon}_{ij}$:

$$\dot{\gamma} = \sqrt{\frac{1}{2} \left(\sum_{i,j} \dot{\epsilon}_{ij} \dot{\epsilon}_{ij} \right)} \quad (4)$$

The velocity equation for drops rising through power law fluids can be written as (see Appendix A for derivation)

$$V = \frac{2}{9n} \frac{(\Delta\rho g)^n r^{n+1}}{K^n X^n} \quad (5)$$

Mhatre and Kintner [1959] found experimentally that the terminal velocity of viscous drops falling through power law fluid is predicted by the apparent Newtonian viscosity of the power law fluid. Crochet et al. [1984] summarizes several approaches described in the literature to determine the values of X for solid spheres as a function of n . More recent work on solid spheres was carried out by Dazhi and Tanner [1985] and Kawase and Moo-Young [1986]. The former also studied how walls of different geometries affect the velocity of spheres. The study of motion of inviscid bubbles in power law fluids started with Astarita and Apuzzo [1965], who used semiquantitative arguments to find the expression for the drag coefficient. Nakano and Tien [1968] found analytically the upper bound of the drag coefficient of a Newtonian spherical drop of variable viscosity moving through a power law fluid of n values up to 1.667 ($m=0.6$). Bhavaraju et al. [1978a, b] found that the ratio between the velocity of a swarm of bubbles and a single bubble increases as n increases. This result was extended to high n values by Chhabra [1988], who found that for $n \geq 2$, swarms of bubbles may rise faster than a single bubble, and for $n=3.33$, bubble swarms may rise twice as fast as a single bubble.

The transfer of the heat or mass of spheres to surrounding power law fluids was studied by Hirose and Moo-Young [1969] and Kawase and Moo-Young [1986, and references therein]. We use here the results obtained by Hirose and Moo-Young [1969] to calculate the heat transfer from the sphere to the ambient fluid. The efficiency of heat (or mass) transfer is usually described as a dependency of the Nusselt number Nu on the Peclet number Pe . Since neither of these parameters depend on the rheologies of the fluids, they retain the same definition for both power law and Newtonian fluids (see notation list). Although the definition of Nu and Pe need not be changed for power law fluids, the relationship between Nu and Pe does need to be corrected by a factor that depends on the only dimensionless parameter in the rheological law, namely, the power law exponent n (see equations (19) and (20)).

Rewriting Known X Values to Fit the Hadamard-Rybczynski Equation

Introduction

The velocity of a viscous sphere rising through power law fluids may be calculated from (5) if the correction factor X is known. The value of X for solid spheres (called X_{sol} here), is a known function of n . Equation (9) and Figure 2 show the polynomial fitting of the values of X_{sol} given by Crochet et al. [1984]. From the Hadamard-Rybczynski equation, the dependency of X on the viscosity ratio for Newtonian fluids ($n = 1$), follows from (2)

$$X(S) = \left(\frac{\mu + 1.5 \mu_{sph}}{\mu + \mu_{sph}} \right) \quad (6)$$

For the limiting cases of a solid sphere falling through power law fluids, and for viscous drops falling through Newtonian fluid, the dependency of X can be extrapolated in a self-consistent way to all values of n and $S = \mu_{sph}/\mu_{eff}$ by

$$V = \frac{1}{3} \frac{\Delta\rho g r^2}{\mu_{eff}} \left(\frac{1}{X_{sol}} \frac{G\mu_{eff} + \mu_{sph}}{(GM\mu_{eff} + 1.5\mu_{sph})} \right)^n \quad (7)$$

where μ_{eff} is the effective viscosity of the ambient power law fluid

$$\mu_{eff} = \frac{K^n 6^{n-1}}{(\Delta\rho g r)^{n-1}} \quad (8)$$

and the parameters X_{sol} , M , and G are functions of $m=1/n$

$$\begin{aligned} X_{sol} &= 1.3 (1-m^2) + m \\ M &= 0.76+0.24m \\ G &= 2.39 - 5.15m + 3.77m^2 \end{aligned} \quad (9)$$

Whereas X_{sol} corrects the velocity for a solid sphere, a combination of X_{sol} , M and G is necessary to correct the velocity of a viscous drop. M and G were obtained by recalculating the data of Nakano and Tien [1968] in order to fit (7) (Figure 2). Values resulting from the multiplication of X_{sol} and M equal 3/2 of the correction factor for the inviscid sphere of Nakano and Tien [1968] (Y in their Figure 1).

Effective viscosity is usually defined by assuming some value of the strain rate. It is impossible to make such an assumption in the case studied here. Instead, it is possible to calculate the characteristic stress $\sigma = \Delta\rho g r$, for the uniaxial condition (1)

$$\mu_{eff} = \frac{\sigma}{\dot{\epsilon}} = \frac{\sigma}{A e^{-E/RT} \sigma^n} = \frac{K^n}{\sigma^{n-1}} = \frac{K^n}{(\Delta\rho g r)^{n-1}} \quad (1)$$

The constant 6^{n-1} that appears in (8) results from our particular geometry and gives a quantitative meaning to our definition of effective viscosity. If we consider a buoyant drop and substitute the ambient power law fluid with a Newtonian fluid with viscosity equal to the effective viscosity calculated in (8), the ascent velocity will remain the same [Mhatre and Kintner, 1959]. This definition of effective viscosity also predicts that the transition of the drop velocity from the solid to the inviscid regime occurs at viscosity contrasts $S=1$, similar to Newtonian fluids (for which S is simply the ratio of Newtonian viscosities).

Equations (5) and (7) are essentially similar; they differ only in the definition of the effective viscosity and in the expansion of X into two terms: X_{sol} and the viscosity-dependent term. Equation (7) reduces to Hadamard-Rybczynski's equation when $n=1$, and it fits the existing data well (Figure 2). There are two advantages of our definition of μ_{eff} : first, there is no need to fix the strain

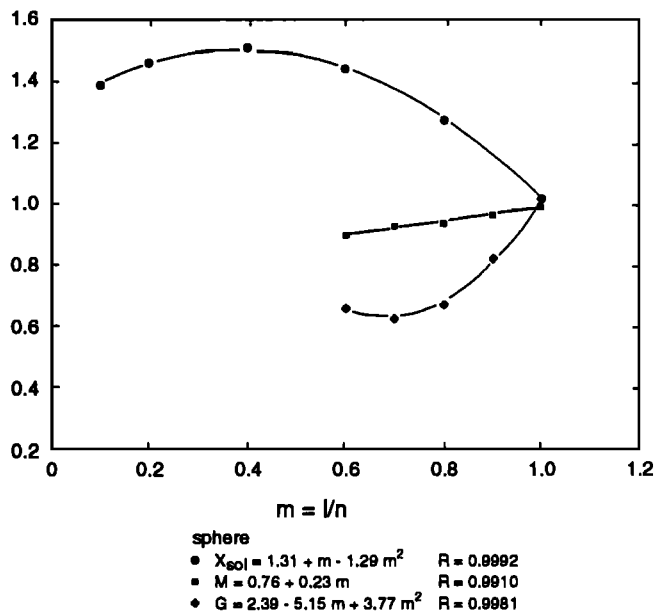


Figure 2. The correction factors for spheres: X_{sol} from Crochet *et al.* [1984] and G and M obtained by the fit of the data of Nakano and Tien [1968] by equation (7).

rate in order to estimate μ_{eff} , and second, the velocity equation is similar to Hadamard-Rybczynski's equation. Since X_{sol} , G , and M always approximate unity, rough estimations of the velocity of natural diapirs may disregard these factors and simply use Hadamard-Rybczynski's equation together with (8).

Procedure for Extrapolation

The values of X for inviscid spheres known from the literature extend only up to $n=1.667$ ($m=0.6$ [Nakano and Tien, 1968]). In order to extend these to geologically interesting values of higher n , we extrapolated the correction values by the same functional dependence (9). Errors due to extrapolation are expected to be only minor due to the shape of the equation and to the small variations in their values. Further research in this area and the derivation of values for these factors to higher n could easily correct our extrapolation.

From Rheological Parameters of Rocks to the Velocity Equation

The geological literature contains several laboratory studies of the rheologies of rocks [e.g., Kirby, 1983; Paterson, 1987; Wilks and Carter, 1990] as well as rheologies of magmas and melts of different compositions at diverse temperatures, pressures and crystal and bubble contents [McBirney and Murase, 1984; Spera *et al.*, 1988]. For simplicity, we assume here that all magmas are Newtonian fluids, and we calculate the value K^n in (7) through the equation

$$K^n = \frac{1}{A e^{-E/RT} 3^{(n+1)/2}} \quad (10)$$

where the values of A in $\text{Pa}^{-n} \text{s}^{-1}$, E in J/mol , and n can be taken directly from the geological literature [e.g., Kirby, 1983].

The velocity of spherical diapiric bodies rising through any power law rock may be calculated by (7), (8), and (10). The next section discusses the influence of ellipticity of the drop on the rising velocity as a function of the power law exponent n . Following that we describe the computer code used to explore the effects of power law rheology and lithospheric temperature gradients on diapiric systems.

Velocity Versus Ellipticity

The correction factors derived above are based on results related to spherical bubbles and drops. Although this work and all previous works that attempted to integrate the rise of diapirs through the lithosphere assume the spherical diapirs [e.g., Marsh, 1982; Miller *et al.*, 1988; Mahon *et al.*, 1988], diapirs may deform as they rise due to heterogeneities of the wall rock properties, interaction with other rising diapirs, asymmetrical thermal aureole around the diapir and, most importantly, the upward increase in viscosity of the wall rock due to temperature decrease. The latter effect causes diapirs to expand laterally on the horizontal plane and to shorten vertically (flat-lying ellipse in Figure 3). In an earlier paper Weinberg [1993] studied the velocity of two-dimensional (2D) solid ellipses rising through power law fluids and showed that the velocity of flat-lying ellipses decreases as n increases, whereas the velocity of ellipses rising parallel to their long axes (upright ellipses), increases. The velocity change with ellipticity is small for aspect ratios up to 2, but increases with n of the ambient fluid. The ratio between the velocity of a solid circle and a flat-lying solid ellipse of such an aspect ratio is 1.5, for $n=3$. Although these 2D results are only qualitatively valid for the 3D case, they are likely to be an upper bound for an oblate flat-lying ellipsoid.

Figure 3 extends the work of Weinberg [1993] to low viscosity flat-lying ellipses and to higher n values, simulating inviscid magmatic diapirs flattened due to the rise through a lithosphere with upward increase in viscosity. The velocities were calculated numerically using a finite difference computer code developed by H. Schmeling and described in Weinberg and Schmeling [1992]. Low-viscosity ellipses show an enhanced difference between the velocity of circles and ellipses as compared to similar results for solid ellipses. However, the velocity decrease is still as small as a factor of 2 when $n=3$ for an ellipse aspect ratio of 2. The influence on velocity of a weak sphere deformation (aspect ratios close to one) can then be assumed to be negligible in our calculations. In the mantle and in the deep crust the isoviscous lines caused by the geothermal gradient have large vertical spacing as compared to the radii of common diapirs. Thus in these regions diapirs may be assumed to be spherical. However, as diapirs rise to shallower crustal levels the vertical distance of isoviscous lines decreases and lateral expansion and vertical flattening of diapirs become

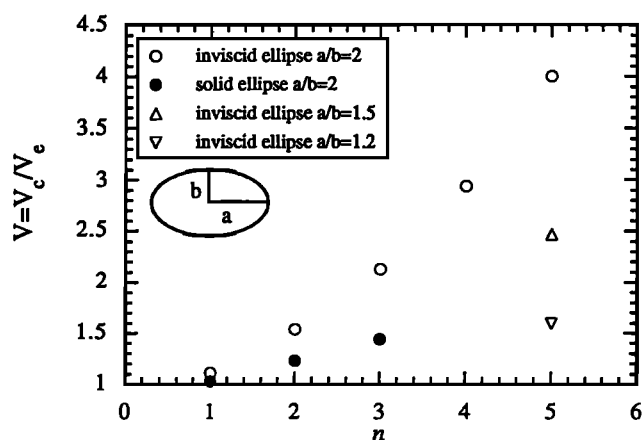


Figure 3. The influence of ellipticity on the velocity of two-dimensional objects rising through power law fluids of different power-law exponents n . The ellipses rise parallel to the short axis as shown in the insert. The velocities are given as the ratio of the velocity of circles (V_c) to that of the ellipse (V_e). "Inviscid ellipses" correspond to ellipses 3 orders of magnitude less viscous than the ambient fluid, and three different ellipticities are shown for $n=5$. "Solid ellipses" correspond to ellipses 3 orders of magnitude more viscous than the ambient fluid [from Weinberg, 1993]. All calculations were carried out for ellipses of equal buoyancy and box width of $5a$ (a is the horizontal axis of the ellipse). Solid ellipses are less influenced by the shape than inviscid ones, and both show that increasing n the influence of the shape on the velocity increases.

more important. At these shallow levels our velocity estimates, calculated below for wall rocks of $n = 3$, may be overestimated by a factor of 2 if their horizontal radius becomes twice that of the vertical radius before the diapir solidifies. However, a deceleration during late stages of emplacement will have very little influence on the depth of solidification of the diapir (see Figure 5).

The calculations carried out below could be improved and correspond more closely to nature if both the shape evolution of the diapir and the correction of diapir's velocity as a function of its shape were known. However, on the basis of the discussion above, we believe that the assumption of a spherical shape will not considerably change our results. We will show that a much more important source of error in the calculations is the relatively high error bar in the determination of the flow law parameters of rocks.

Computer Code

A computer code was developed in order to integrate the velocity equation for the ascent of spherical (or cylindrical) diapirs through the lithosphere. The ascent rate of the diapir considered here is controlled by 10 variables. Four of these were chosen to be the characteristic dimensions

$$t^* = H^2 / k$$

$$L^* = H$$

$$\rho^* = \Delta\rho$$

$$T^* = E / R$$

The remaining six variables (geothermal gradient dT/dH , T_{sol} , g , r , K^n , and n) were used to form six independent dimensionless numbers that control the final depth of crystallization of the diapir:

the compositional Rayleigh number Ra modified here for power law fluid

$$Ra = \frac{(\Delta\rho g r)^n r H}{k K^n \delta^{n-1}}$$

where

$$K^n = \frac{1}{3^{n+1/2} A}$$

the dimensionless geothermal gradient gt

$$gt = \frac{\partial T}{\partial H} \frac{HR}{E}$$

the effective viscosity of the sphere

$$\mu'_{sph} = \frac{\mu_{sph} k}{\Delta\rho g r H^2}$$

the solidus temperature

$$T'_{sol} = T_{sol} R/E$$

and the radius $r'=r/H$, and n .

Table 1. Parameters Controlling the Ascent of the Tara Granodiorite

	Tara Granodiorite
r (km)	3.0
H (km)	25.0
T_{init} magma ($^{\circ}\text{C}$)	770 \pm 30
T_{sol} ($^{\circ}\text{C}$)	650
k (m^2/s)	7 $\times 10^{-7}$
$\Delta\rho$ (kg/m^3)	550
Geothermal gradient ($^{\circ}\text{C}/\text{km}$)	30
E (kJ/mol)	142
A (MPa^{-n}/s)	2 $\times 10^{-4}$
n	2.0

Parameters are from Miller *et al.* [1988]. The values of E , A , and n are from Westerly granite [Hansen and Carter, 1982]

The code considers the effect of heat softening of the wall rock on the velocity and calculates the cooling of the diapir at each ascent step (a detailed description of the code and the equations used is given in Appendix B). We studied systematic variations in five of the six dimensionless parameters that control ascent and depth of solidification of the diapir. We did not study μ'_{sph} because the diapir was assumed to have a viscosity well below that of the wall rock, behaving as an inviscid body. Results fit by the least squares method are presented in Appendix C in the form of an equation that allows calculation of the depth of solidification as a function of all five parameters. To

illustrate the use of the program, and to give an idea of the dependence of solidification depth on the several parameters, results for relatively well-known geological systems are presented below.

Application to Selected Geological Systems The Tara Granodiorite

As a first example, we simulate the ascent of the Tara granodiorite through the Cootlantra granodiorite in southeastern Australia [Miller *et al.*, 1988]. We chose this diapir because the parameters controlling its ascent are relatively well constrained (Table 1). Figures 4a-4c show

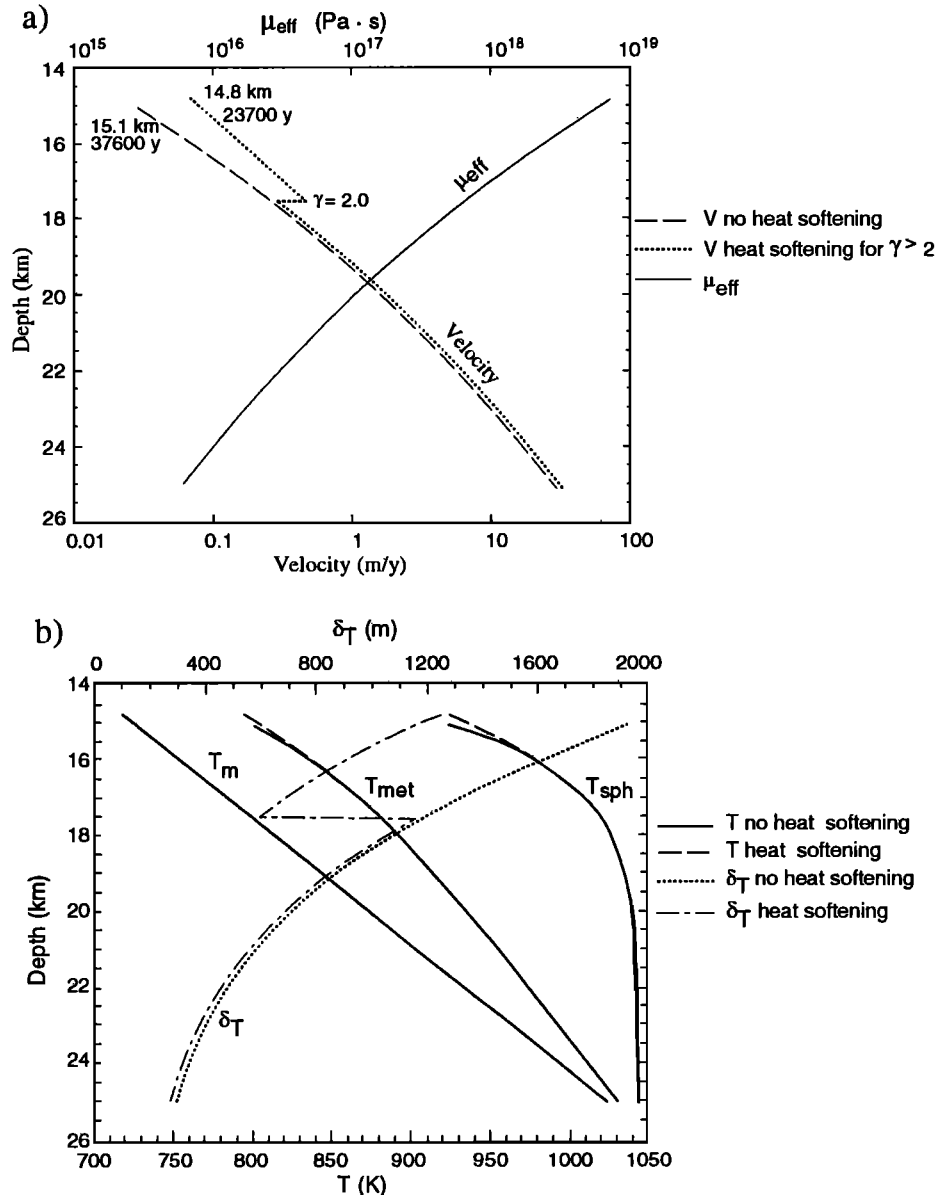


Figure 4. (a) Velocity and effective viscosity of the wall rock μ_{eff} for spheres rising with and without thermal softening of the ambient rock and constant density contrast. Calculation of μ_{eff} is based on (8) using the regional temperature at the diapir's depth and ignoring softening due to heat released by the diapir. Thermal softening of the wall rock is included in the calculation of drag reduction. (b) Regional temperature (T), temperature of the sphere (T_{sph}), thickness of the metamorphic aureole (δ_t), and aureole temperature (T_{met}) as a function of depth. The viscosity of the sphere increases as it rises, but is always sufficiently lower than that of its wall rocks for it to be considered inviscid. (c) Pe and Dr .

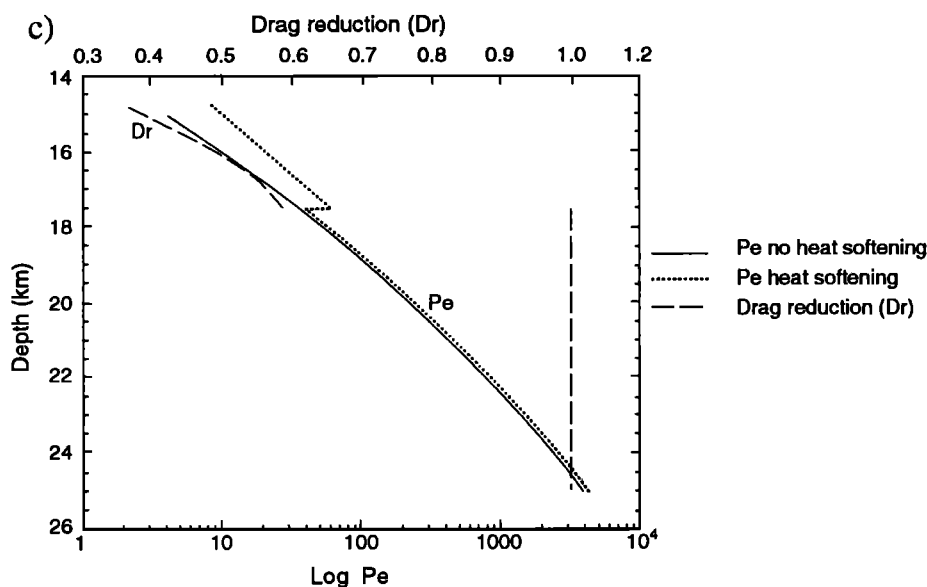


Fig. 4. (continued)

the results of calculations for two cases, one in which the rise rate is corrected for thermal softening of the wall rock and one without such corrections. Both diapirs rise from a starting depth of 25 km at 28 m/yr but rapidly decelerate following the same evolutionary path (Figure 4a-4c) until $\gamma=2$. At this point, the code starts to calculate the drag reduction (Dr) for the thermally softened case, causing the abrupt acceleration at a depth of 17.5 km (Figure 4c). This unnatural jump arises only because of the absence of solutions for Dr when $\gamma < 2$. In nature the velocities of the two cases are expected to gradually diverge, so that the thermally-softened case finally crystallizes at a slightly more shallow depth than predicted here. The depth of solidification of both diapirs (i.e., when $T_{sph} = T_{sol} = 650^\circ\text{C}$) is around 15 km, and the thermally softened case rises only 300 m further than that without thermal softening (Figure 4a).

The diapir rises significantly more slowly at higher crustal levels, as μ_{eff} increases, with decreasing T (Figure 4a). Two thirds of the total ascent time is spent in rising the last 3 km before solidification. The temperature profile of the crust and diapir (T and T_{sph} , respectively), and the thickness and temperatures of the metamorphic aureole (δ_t and T_{met} , respectively) are summarized in Figure 4b. During the first 5000 years the diapir cools 25°C as it ascends 7.5 km through a crust cooling according to the geothermal gradient (in degrees Celsius per kilometer). The maximum temperature difference is 230°C at a depth of 17 km. From then on, the diapir cools at approximately the same rate as the geothermal gradient but is 210°C warmer than its wall rocks, and it eventually solidifies at a depth of 15 km. The diapir rises so fast through rocks so hot in the first 7-8 km of ascent that it loses very little heat. As the diapir slows at higher crustal levels, the cooling rate per risen meter increases and the metamorphic aureole widens considerably (δ_t , Figure 4b). At this stage, Pe decreases below 100 and thermal softening becomes more and more important (decrease in Dr , Figure 4c). Eventually, the diapir solidifies and all its remaining heat is conducted to the wall rock, causing

maximum thermal disturbance.

The unrealistically high Pe just before solidification (Figure 4c) results from the constant density difference $\Delta\rho$ used throughout the calculation. In nature, $\Delta\rho$ is expected to decrease as the cooling magma crystallizes. To illustrate this, we calculated the ascent of the same diapir but with a linear decrease in $\Delta\rho$ from 550 kg/m^3 to zero at solidification (Figure 5). Comparison between Figures 4a and 5 shows that lower Pe leads to solidification occurring 500 m deeper after slower ascent and that thermal softening becomes more important at final emplacement.

Systematic study of the way in which various parameters control the depth of solidification of a Tara-like granodiorite was carried out by varying one parameter and keeping all others constant as in Table 1 (Figure 6). Changes in the two values controlling the buoyancy of the diapir have little influence (Figure 6a) but, as is clear from (7), the radius r is more important than $\Delta\rho$. The logarithmic shape of the dependencies indicates increased control of buoyancy on the solidification depth. Initial and solidus temperature of the magma also have little influence on the solidification depth (Figure 6b).

The main parameters controlling the solidification depth are A , E , and n (Figures 6c and 6d). All three parameters were varied here by the uncertainties of the values obtained in laboratory experiments (for example, see the rheology of olivine of Kirby [1983]). Increasing n has little effect but leads to shallower emplacement for the Tara-like granodiorite. The most important controls on the depth of solidification studied here are A and E . A likely span for the preexponential parameter A causes changes in the final pluton depth of nearly 5 km, whereas the activation energy E changes it by nearly 16 km. At one extreme of E , the diapir hardly leaves its source; at the other extreme the diapir almost reaches the surface. Miller *et al.* [1988] estimated the solidification depth of the Tara granodiorite to 10-12 km. As demonstrated above, this depth can easily be obtained by adjusting slightly the values of the rheological properties of the wall rock (the Westerly granite).

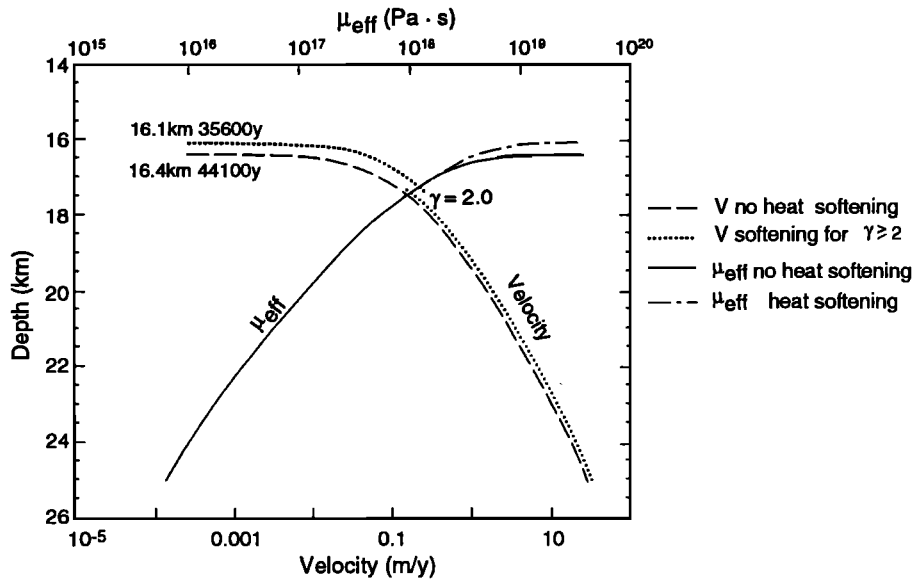


Figure 5. V and μ_{eff} for spheres rising with and without thermal softening of the ambient rock where $\Delta\rho$ decreases linearly from 550 kg/m^3 to zero just before solidification.

Diapiric Ascent From a Subducting Slab

This calculation is a simplified model of the rise of a batch of basic magma from a subducting slab. The batch rises through the overlying mantle to underplate light continental crust below the Moho. The arrival of the mafic magma at the Moho melts a smaller silicic diapir which ascends through the continental crust. The

parameters used in the calculations are listed in Table 2. In the first 60 km we use the geothermal gradient of the mantle and the rheology of olivine [Kirby, 1983]. The continental crust is 40 km thick and divided into two layers: a lower 15 km formed by Adirondacks granulite (rheology given by Wilks and Carter [1990]) and an upper 25 km of Westerly granite (rheology given in Hansen and Carter [1982]).

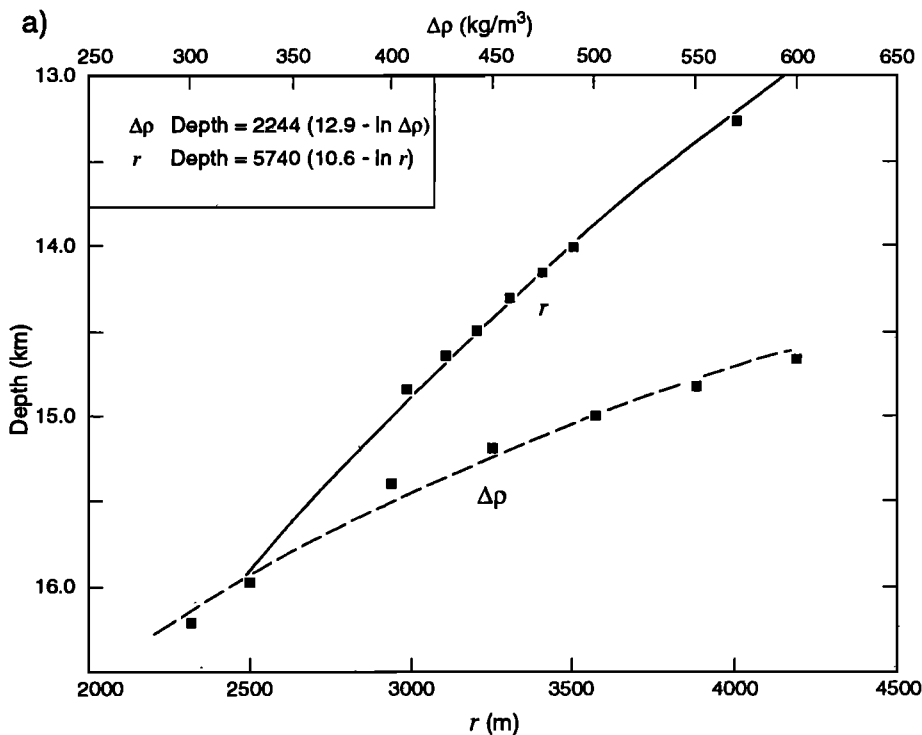


Figure 6. Systematic variation of parameters controlling the depth of emplacement of a Tara-like granodiorite: (a) r and $\Delta\rho$, (b) initial and solidus temperature (T_{init} and T_{sol} , respectively), (c) E and A , and (d) n . Each parameter was varied individually while the others were kept constant (see Table 1).

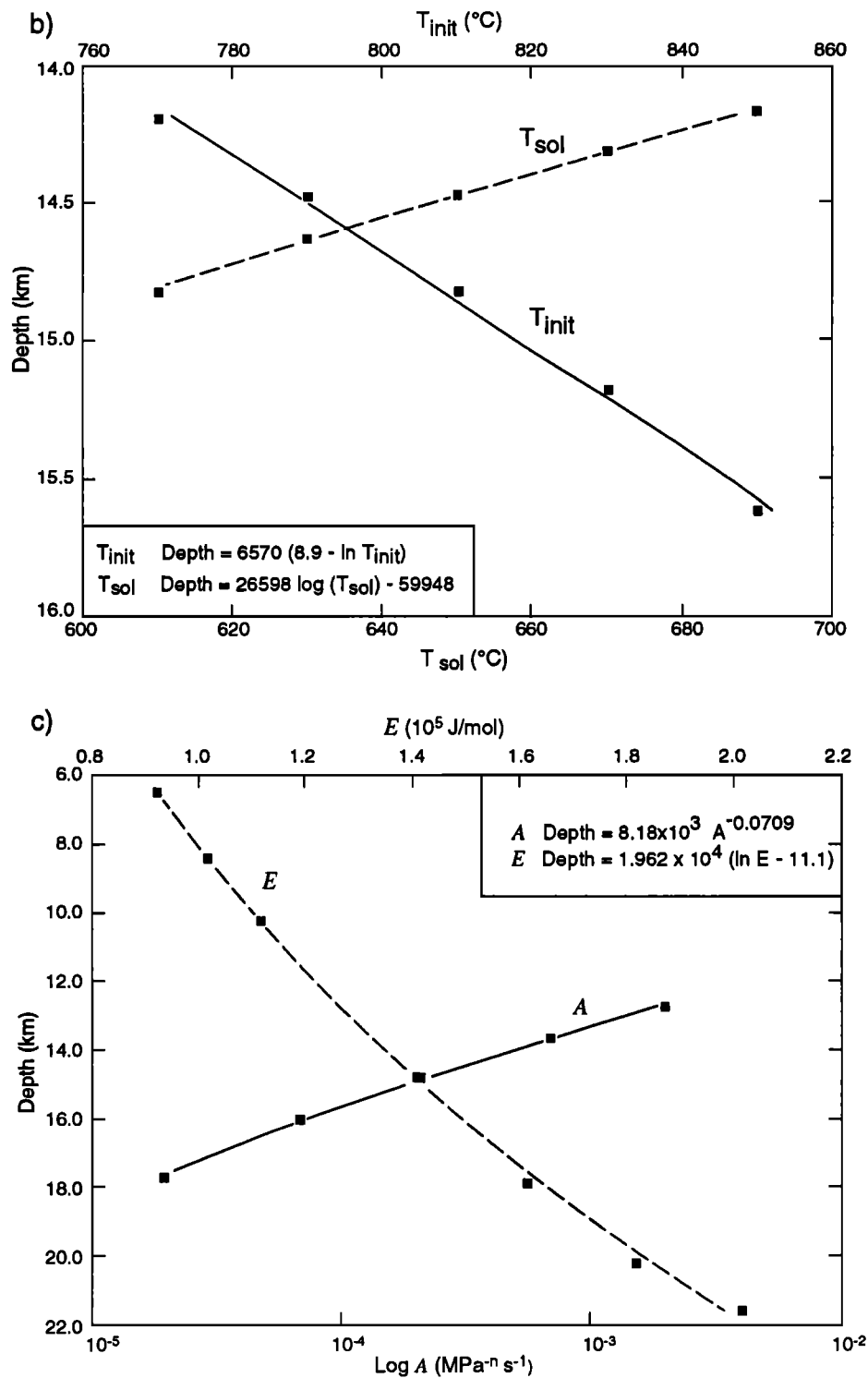


Fig. 6. (continued)

In this calculation we have not built in any pause between the arrival of the mantle diapir at the Moho and the departure of the crustal silicic diapir; instead, the diapir is assumed to rise straight through the Moho despite its change in chemistry. The appropriate pause could be added to the total ascent time if its duration were known. Although *Huppert and Sparks* [1988] calculated that it would take 10^2 - 10^3 years for a basic magma to melt a layer at the bottom of the crust, the incubation time taken

by this layer to initiate its ascent as a Rayleigh-Taylor instability is unknown and could be similar to the total ascent time.

The results for this system (Figure 7) show a diapir rising through 60 km of mantle in 0.18 m.y. (Figure 7a) and reaching the base of the crust 167 K warmer than the surrounding temperature (Figure 7b). It then melts a volume of acidic magma that rises as a sphere of 4 km radius (melting process is not considered) that rises in 0.17

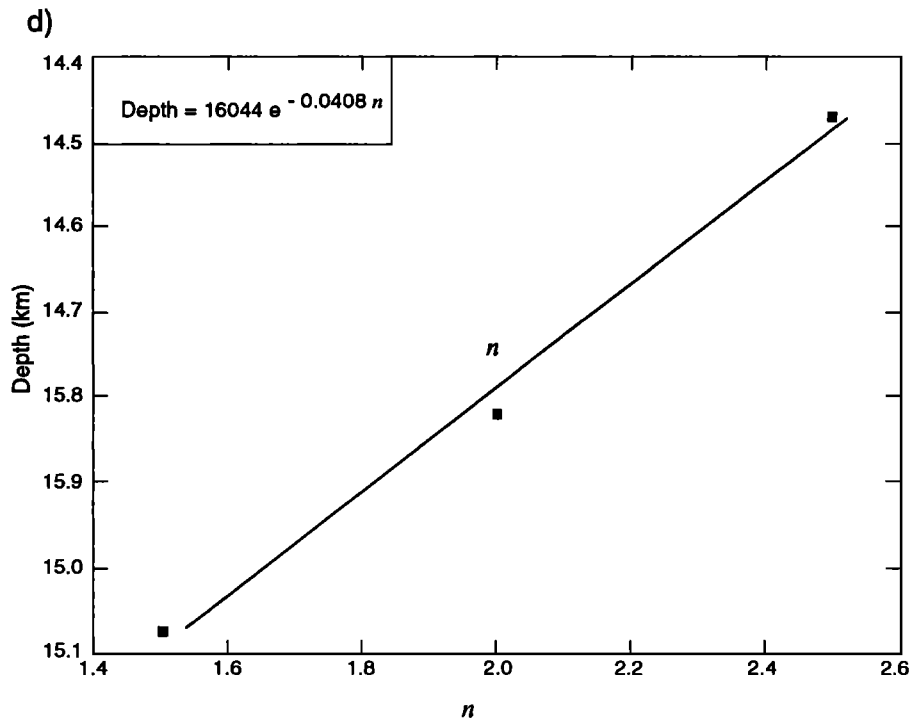


Fig. 6. (continued)

m.y. to a depth of 15.8 km, where it solidifies. Two jumps in the velocity can be seen in Figure 7a. The first corresponds to the change from mantle to lower crustal diapir at a depth of 40 km, and the second corresponds to the change in rheology from granulite to Westerly granite at a depth of 25 km. Despite the decrease in density contrast the sphere rises through the granite 1000 times faster than through the granulite at the transition depth. This is because effective viscosity of the granite is low compared to the granulite at the same temperature (Figure

7a). A smaller jump also occurs in each rock type, every time γ becomes ≥ 2.0 , and Dr begins to affect the ascent velocity (Figure 7c).

Discussion

All the results presented here refer to diapirs rising in the absence of external tectonic stresses. Such stresses could considerably affect our conclusions and change the ascent velocity, depth of solidification, and shape of the body.

Table 2. Parameters Controlling the Ascent of a Mantle Diapir That Melts a Continental Crustal Diapir

	Mantle Diapir	Lower Crust (Adirondacks Granulite)	Upper Crust (Westerly Granite)
r (km)	10.0	5.0	5.0
H (km)	100.0	40.0	25.0
T_{init} magma ($^{\circ}\text{C}$)	1302	1001	
T_{sol} magma ($^{\circ}\text{C}$)	850	650	650
k (m^2/s)	10^{-6}	10^{-6}	10^{-6}
$\Delta\rho$ (kg/m^3)	500	500	400
Geothermal gradient ($^{\circ}\text{C}/\text{km}$)	5	25	25
E (kJ/mol)	533	243	142
A (MPa^{-n}/s)	6.34×10^4	8×10^{-3}	2×10^{-4}
n	3.5	3.1	2.0

Values of E , A , and n for the mantle are averages for olivine from Kirby [1983], Adirondacks granulite from Wilks and Carter [1990] simulates the lower crust and Westerly granite from Hansen and Carter [1982] the upper crust.

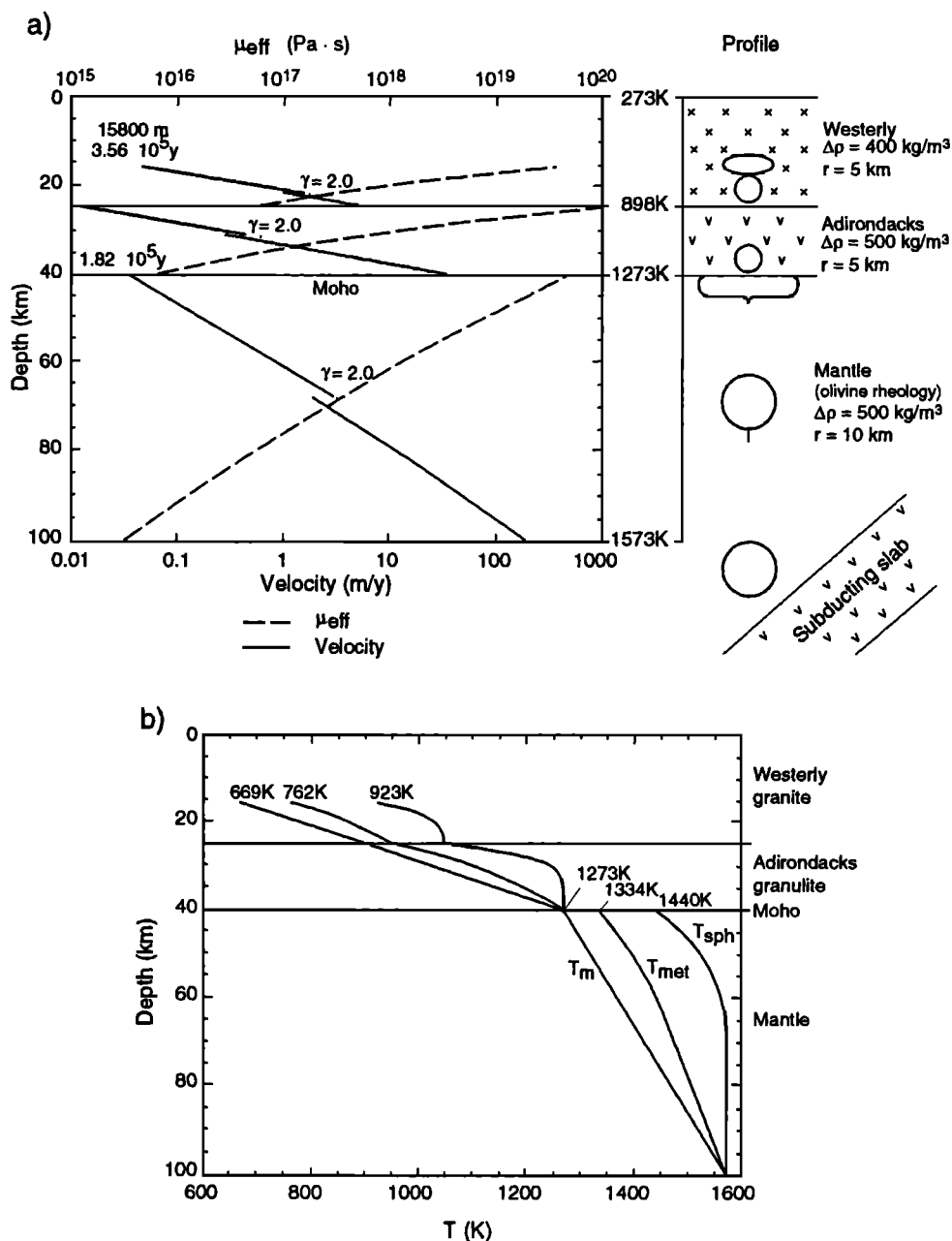


Figure 7. A diapir rises from a subducting slab through a mantle with olivine rheology. At its arrival at the Moho, the mantle diapir melts a smaller crustal diapir which then rises through a layered crust formed by Adirondacks granulite at the base and by Westerly granite at the top. (a) Velocity and μ_{eff} as a function of depth, (b) T_{sph} , T_m and T_{met} , (c) drag reduction Dr when $\gamma \geq 2$; for smaller γ values, $Dr=1$.

Time and Velocity Constraints

The velocity and time taken for diapiric ascent derived here fit the few geological constraints available reasonably well. *Mahon et al.* [1988] argue that granitoid diapirs have to ascend in more than 10^4 years and less than 10^5 years. This is because it takes more than 10^4 years for thermal softening of the wall rock to be effective, and less than 10^5 years for large diapirs to solidify. This work shows that strain rate is so much more important than thermal softening as to render the lower limit of 10^4 years hardly

significant. The upper time limit is in accord with the solidification time of the diapirs modeled here. *Marsh* [1982] found that in the subduction zone beneath Scotia, the response time of volcanism to a young subducting plate is 1 m.y. He argued that the viscosity of the wall rocks in contact with the diapir needs to be 10^{17} to 10^{18} Pa s for diapirism to occur within reasonable times. Our calculations did not consider the time to produce batches of crustal magma from the mantle magma. Nonetheless, the diapirs took a very reasonable 0.35 m.y. to rise from source to 15 km from the surface. The effective viscosity of the wall rock approximates the requirements of Marsh's

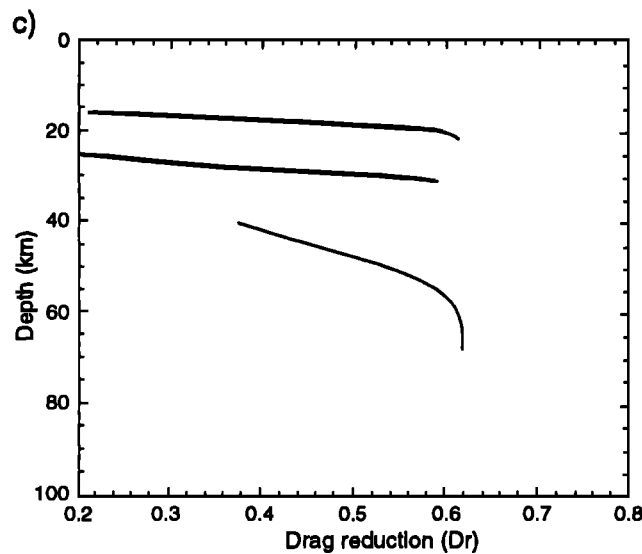


Fig. 7. (continued)

calculations (Figure 7a). A diapir formed near the subducting lithosphere must rise faster than 3cm/yr in order not to be dragged deeper into the mantle with the descending plate [Marsh 1979]. The mantle diapir has an initial velocity of 190 m/yr, for the parameters in Table 2 (Figure 7), and only diapirs having a radius smaller than 1.4 km would be dragged downward by the subducting plate. To form such large magma bodies, shearing along the top of the subducting plate (and in the overlying mantle wedge) and consequent disruption of magma batches into small bodies have to be slower than the processes of melting and accumulation of magmas.

The depth of solidification of a diapir may differ from that calculated above if (1) the rheological parameters are slightly different, (2) two or more diapirs follow the same path (see Marsh [1982] for hot-Stokes models), (3) a swarm of diapirs rise simultaneously (faster ascent rates [see Chhabra, 1988]), and/or (4) a rigid top boundary is present.

Thermal Aureole

In order for diapiric ascent to occur at practical rates, Marsh [1982] invoked in his hot-Stokes models warming of the country rocks to their solidus temperature. Paterson *et al.* [1991] argued against diapirism based on the lack of extensive migmatites around most upper and mid crustal plutons. However, we have shown here that strain rate softening of the wall rock is an effective substitute for thermal softening. There is therefore no need to expect wide aureoles of migmatites around diapirs.

Magma Transport Through Fractures

Most recent challenges on the diapiric ascent of magmas have been based mainly on the absence of a sound theory that explains how diapirs can ascend through stiff lithospheric rocks in geologically reasonable times [e.g.,

Bateman, 1984; Paterson *et al.*, 1991; Clemens and Mawer, 1992]. The low ascent rates of diapirs in previous calculations make the ascent of magmas through fractures a clearly more effective transport mechanism. Here we will discuss some difficulties related to fracturing due to buoyancy forces and compare the relative effectiveness of magma transport by the two mechanisms.

Beris *et al.* [1985] showed that for a sphere to rise through Bingham fluids, the dimensionless group Y_g , corresponding to the ratio of the yield stress to the external force acting on the sphere, has to be smaller than 0.143:

$$Y_g = \frac{2\tau_y \pi r^2}{\frac{4}{3} \pi \Delta \rho r^3 g} = \frac{3}{2} \frac{\tau_y}{\Delta \rho g r} \leq 0.143 \quad (11)$$

where τ_y is the yield stress for the ambient rocks. For normal stresses $\sigma_n = \rho g H$ (lithostatic pressure) of 200 - 2000 MPa

$$\tau_y = 50 + 0.6\sigma_n \quad (12)$$

where τ_y is the yield stress [Byerlee, 1978]. Substituting (11) in (12) yields

$$\Delta \rho g r \geq \frac{50 + 0.6 \rho g H}{0.0953}$$

Thus, in order for the diapir to move at all, its buoyancy stress has to be approximately 6 times larger than the normal stress measured at the center of the body. It is clear that the diapir will not move through a plastic fluid if its buoyancy does not exceed the yield strength. Extremely large magma bodies, high pore pressure, proximity to a free surface, external regional stresses, or concentration of these regional stresses at the tip of a dike must be invoked in order for the rise through fracturing to be possible.

Clemens and Mawer [1992] offered transport of magma through self-propagating fractures as an alternative to diapirism. However, a dike cools much faster than a

sphere of the same volume. *Marsh and Kantha* [1978] concluded that for a given volume of magma to reach the same depth, it must travel 10^4 times faster in a dike than in a spherical diapir. Our results suggest that diapiric ascent rates of 10-50 m/yr may be common in the lower crust. Such velocities are 1 order of magnitude more efficient in transporting magma at 3×10^4 m/yr along a 1-km-long and 3-m-thick dike [from *Clemens and Mawer*, 1992, p. 349]. However, as the diapir rises and decelerates, fracturing becomes easier due to decreased lithostatic pressure (σ_n) and may at a certain critical point become more efficient in transporting magma than diapirism. It is possible that at a certain depth the system changes from diapirism to fracturing [Rubin, 1993].

Another argument used against diapirs of buoyant magma [e.g., *Clemens and Mawer*, 1992] is the nature of the structures in experiments carried out by *Ramberg* [1981], where low-viscosity model magmas rose through high-viscosity overburden. However, it is known from Hadamard-Rybczynski equation (2) and confirmed by (7) that diapirs more than 10^2 times less viscous than the wall rock will behave like inviscid bubbles, and further decrease in viscosity will not alter the behavior. The structures observed by *Ramberg* [1981, pp. 333-340] result not from the low viscosity of the model magmas, but from their enormous volumes. In *Ramberg's* experiment M, the "magma body" had the volume of a sphere with a diameter equivalent to two thirds of the total thickness of his model "crust". The resulting fracturing of his model crust and the disruption of the initial "magma body", on the one hand proves the above statement that diapirs cannot overcome the moving criterion for spheres in Bingham fluids (11), and on the other hand shows that fracturing is preferable only for such large magma bodies and close to a free surface. *Ramberg's* model cannot be directly extrapolated for smaller bodies deep in the crust or lithosphere.

Comparison Between Hot-Stokes and Power Law Models

Thermal softening of the ambient rocks (hot-Stokes models) has surprisingly little influence in the rate of rise of a normal-sized diapir. Thermal softening is negligible during the initial stages of ascent because the temperature contrast between diapir and country rocks is usually small (low γ values). By contrast, strain rate softening allows the diapir to rise so fast that it loses very little heat while ascending. As the warm diapir reaches the cooler crust, γ increases and viscous drag starts to decrease due to thermal softening. However, this occurs only when the diapir is close to its final solidification level, and its thermal energy is rapidly lost due to the slow ascent rates. The diapir may still be buoyant when it solidifies, and the high temperature difference between it and its wall rock, and its low Pe , may considerably reduce drag so that the crystalline diapir rises considerably faster than expected without thermal softening effects.

Conclusions

This work has expressed the velocity of spherical drops rising through power law fluids in the form of Hadamard-Rybczynski's equation. The correction factors X_{sol} , G ,

and M calculated from known results for drops were extrapolated to high n values and then applied to geological systems. The most important advantages of our equations (7) and (8) are that with our definition of the effective viscosity (8), the velocity equation becomes similar to Hadamard-Rybczynski's equation; the known values of the rheology of rocks can be directly applied to calculate the effective viscosity of the wall rock (μ_{eff}); it is not necessary to assume a strain rate in order to calculate μ_{eff} , instead the buoyancy stress of the diapir is used; and since the correction factors are always close to unity, the velocity may be approximated by calculating μ_{eff} and using Hadamard-Rybczynski's equation. Any errors arising from the extrapolation of the correction factors to high n may be remedied when these factors are eventually determined for high n values. More important sources of error are the uncertainties concerning the rheologies of rocks [Paterson, 1987]. We have shown that the rheological parameters A and E are the main variables controlling the depth at which a diapir solidifies. Improved knowledge of these parameters will considerably deepen our understanding of crustal diapirs and allow more accurate predictions of their development.

The high velocities calculated here result from our definition of μ_{eff} . Diapirs are able to rise faster through power law fluids than through Newtonian fluids, and such fast rise is not accompanied by large heat loss (the main problem with the hot-Stokes models). Thus diapirs are emplaced at much higher levels than earlier predicted, and their thermal energy eases late stages of ascent. Thermal softening of the wall rocks has never been considered adequate to account for granite plutons reaching high crustal levels. Earlier workers had difficulties in accounting for the way in which hot-Stokes diapirs rise more than a few radii before solidifying. We have shown that thermal softening has little effect on the depth of solidification of a diapir and that strain rate softening of power law rocks is a far more effective alternative, allowing magmatic diapirs to ascend sufficiently fast to reach depths of 10-15 km.

In summary, instead of assuming a strain rate in advance as has been usual in the past, we use the buoyancy stress of the sphere and the rheological parameters of rocks to calculate a more realistic effective viscosity of the wall rock. Diapirs may thus transport large quantities of melt efficiently through power law mantle and crust without needing to heat their wall rocks to solidus temperatures.

Appendix A: Velocity Equation for Settling Spheres Through Power Law Fluids

A convenient way to study the rate of translation of a drop through power law fluids is to measure how much it deviates from the expected rate of translation through Newtonian fluids. This is usually done by measuring the difference in the drag force (D) exerted on the sphere by its viscous surroundings, in terms of the dimensionless drag coefficient (C_D)

$$C_D = \frac{8D}{\rho V^2 \pi (2r)^2} \quad (A1)$$

The Hadamard-Rybczynski equation shows that the drag coefficient C_D for a viscous drop moving slowly through a Newtonian fluid is

$$C_D = \frac{24}{Re} \left(\frac{\mu + 1.5 \mu_{sph}}{\mu + \mu_{sph}} \right) \quad (A2)$$

where

$$Re = \frac{2rV}{\mu} \quad (A3)$$

For power law fluids, C_D and Re must be redefined as [Crochet *et al.*, 1984]

$$C_D = \left(\frac{24}{Re} \right) X \quad (A4)$$

$$Re = \frac{2^m r^m V^{2-m} \rho}{K} \quad (A5)$$

where X is a correction factor that depends on n and the viscosity ratio between the drop and the ambient fluid. For solid spheres in Newtonian ambient fluids, $X=1$, and for a drop of any viscosity (from (A2))

$$X = \frac{1 + 1.5S}{1 + S}$$

where $S = \mu_{sph}/\mu$. X also describes the influence of nonlinearity for the more general case (n or $m \neq 1$).

Several workers have determined the drag coefficient C_D for spheres translating through power law fluids [e.g., Crochet *et al.*, 1984]. Once C_D is known, the velocity equation of a sphere can be written by setting the drag force equal to the buoyancy force

$$D = \frac{4}{3} \pi r^3 \Delta \rho g \quad (A6)$$

and substituting D in (A1) and then in (A4), with Re defined as in (A5). Reorganizing, we obtain the equation for the velocity of a buoyant spherical drop rising through a power law fluid

$$V = \frac{2}{9^n} \frac{(\Delta \rho g)^n r^{n+1}}{K^n X^n} \quad (A7)$$

(A7) reduces to Hadamard-Rybczynski equation (2) when $n=1$.

Appendix B: The Computer Code "Rise"

The computer code "Rise" starts by reading the six dimensionless parameters that control diapiric ascent and calculates the effective viscosity of the wall rock μ_{eff} given the buoyancy stress due to the diapir and the temperature of the ambient rock and diapir (assumed initially to be the same). The program assumes a uniform temperature inside the sphere when it calculates the velocity of the top (or

center) of the body. After calculating μ_{eff} , the program then calculates the velocity of the sphere, its Peclet number (Pe) and the distance in front of the sphere where the temperature decays to $1/e$ of the temperature at the sphere's surface (δ_T as defined by Daly and Raefsky [1985]). The dimensionless relationships used by the program are

$$\mu'_{eff} = \frac{r'}{Ra e^{(-1/T')}} \quad (B1)$$

$$V' = \frac{Ra e^{(-1/T')}}{3} \left(\frac{\mu'_{eff} G + \mu'_{sph}}{X_{sol}(GM\mu'_{eff} + 1.5\mu'_{sph})} \right)^n$$

$$Pe = V'r' \quad (B1)$$

The Nusselt number (Nu) for an inviscid diapir (very small S) is calculated by using the equation for a Newtonian ambient fluid given by Daly and Raefsky [1985, equation 25], corrected by the factor Y_M for power law fluids given by Hirose and Moo-Young [1969]

$$Nu = 0.795 + 0.459 Y_M Pe^{1/2} \quad (B2)$$

where

$$Y_M = \left(1 - \frac{4m(m-1)}{(2m-1)} \right)^{1/2} \quad (B3)$$

We chose not to use the whole equation for Nu given in Hirose and Moo-Young [1969] because, when used for a Newtonian ambient fluid, their solution is not in accordance with that established in Levich [1962] and corrected in Daly and Raefsky [1985].

The velocity in (B1) does not take account of the drag reduction due to softening of the wall rocks caused by heat released from the rising diapir. Thus the program corrects the velocity in (B1) and the Nu in (B2) for the drag reduction, according to the results obtained by Daly and Raefsky [1985]. Although their solution was derived for ambient Newtonian fluids, we believe it to be a good approximation even for power law wall rocks. This is because the length scale of thermal softening (fraction of a radius) is much smaller than the length scale of strain rate softening (a few radii). No drag reduction is applied in the first step, since the temperature contrast between the diapir and its wall rock is likely to be low during initial ascent. The program calculates γ for every subsequent step; γ is defined as \log_{10} of the total viscosity variation due to the temperature gradient from the surface of the diapir to the temperature of the ambient fluid at infinity [Daly and Raefsky, 1985]

$$\gamma = \log_{10} e^{-1/(T'_{sph}-T')} \quad (B4)$$

Daly and Raefsky's solution is limited to values of $\gamma \geq 2$, so for γ greater than this value the program calculates the parameter Δ and the drag reduction, Dr , using

$$\Delta = \epsilon Nu$$

$$Dr = \frac{0.62\Delta}{0.60 + \Delta} \quad (B5)$$

where

$$\varepsilon = \gamma^3 10^{-7}$$

and

$$Nu = 0.795 + 0.459 Y_M (Pe \varepsilon^{-0.2})^{1/2}$$

and divides the velocity from (7) by Dr . Drag reduction is important only when Pe is between 1 and 100 [Daly and Raefsky, 1985], and it will be shown later that these values occur only when the diapir is close to its final emplacement level.

At every step, cooling of the sphere and its new temperature is calculated according to [from Marsh and Kantha, 1978]

$$dT = - \frac{3Nu (T'_{sph} - T) dt}{r^2} \text{ for sphere.} \quad (B6)$$

The program assumes uniform temperature rather than the complex crystallization processes in a natural diapir. When the temperature of the rising body achieves $1.1 T'_{sol}$, its viscosity begins to increase and it eventually rises 10 orders of magnitude just before total crystallization [Cruden, 1990]. If the diapir loses its buoyancy by crystallizing (when $T'_s = T'_{sol}$), the program stops calculating.

Appendix C: Solidification Depth of a Diapir

The results of calculations for the depth of solidification H of a diapir as a function of the five dimensionless parameters have been fit by the least squares method. The following equation fits the numerical results with a maximum relative error of 5.6% (calculated by the difference of predicted and calculated values divided by the sum of both)

$$H = 0.6434 - 0.1444gt - 0.2279Ra + 0.0464Ra \cdot gt + 0.1316T'_{sol} - 0.0404 T'_{sol} gt - 0.0632T'_{sol} Ra + 0.0192T'_{sol} Ra gt + 0.0455n - 0.0218n gt - 0.0074n Ra + 0.0049n Ra gt - 0.0271n T'_{sol} + 0.0118n T'_{sol} gt + 0.0142n T'_{sol} Ra - 0.0062n T'_{sol} Ra gt + 0.0573r - 0.0253r gt - 0.0336r Ra + 0.0137r Ra gt - 0.0226r T'_{sol} + 0.0050r T'_{sol} gt + 0.0110r T'_{sol} Ra - 0.0024r T'_{sol} Ra \cdot gt - 0.0226r n + 0.0111r n gt + 0.0090r n Ra - 0.0045r n Ra gt + 0.0115r n T'_{sol} - 0.0042r n T'_{sol} gt - 0.0059r n T'_{sol} Ra + 0.0022r n T'_{sol} Ra gt$$

Notation

A	preexponential parameter, $\text{Pa}^{-n} \text{s}^{-1}$
C_D	dimensionless drag coefficient
Dr	drag reduction caused by thermal softening
E	activation energy, J/mol
g	acceleration due to gravity

gt	dimensionless geothermal gradient ($dT/dx HR/E$)
G	correction factor function of n , defined in (9)
H	depth of the top of the diapir
K	$\sigma/\dot{\varepsilon}^{1/n}$ in $\text{Pa s}^{1/n}$, uniaxial case
k	thermal diffusivity
L^*	length scaling parameter
m	$1/n$
M	correction factor function of n , defined in (9)
n	power law exponent
Nu	Nusselt number, $qr/\lambda (T'_{sph} - T)$
Pe	Peclet number (Vr/k)
q	heat flux out of the hot sphere
R	gas constant, 8.314 J/mol K
r	sphere radius
r'	dimensionless radius ($r' = r/H$)
Re	Reynolds number defined in (A3) and (A5)
Ra	compositional Rayleigh number, $(\Delta\rho g r)^n r H / K^n k 6^{n-1}$
S	μ_{sph} / μ_{eff}
t	time
dt	time step in numerical calculations
dT	temperature decay of the sphere per time step (dt)
T	temperature (without any subscript corresponds to the wall rock or ambient fluid)
T'	dimensionless solidus temperature
V	sphere's or diapir's velocity
w	width of the box used in numerical calculations
w'	dimensionless width (w/r)
X	correction factor
$X(n)$	correction factor function of n and μ_{sph}/μ_{eff}
Y_g	the ratio of the yield stress to the external force acting on the sphere, defined in (11)
Y_M	correction for Nu of power law fluids, defined in (B3)

Greek symbols

γ	\log_{10} of the total viscosity variation in (B4) [Daly and Raefsky, 1985]
$\dot{\gamma}$	second invariant of the strain rate tensor $\dot{\varepsilon}_{ij}$
Δ	defined in (B5) from Daly and Raefsky [1985]
δ_t	thickness of the metamorphic aureole
$\dot{\varepsilon}$	uniaxial strain rate
$\dot{\varepsilon}_{ij}$	strain rate tensor
λ	heat conductivity
μ	viscosity of the Newtonian ambient fluid
μ_{eff}	effective viscosity of the ambient fluid defined

by	(8)
μ'_{sph}	dimensionless viscosity of the sphere, $\mu'_{\text{sph}} = (\mu_{\text{sph}} k)/(\Delta\rho g r H^2)$
$\Delta\rho$	density difference ($\rho - \rho_{\text{sph}}$)
σ	uniaxial stress
σ_{ij}	stress tensor
σ_n	lithostatic pressure $\sigma_n = \rho g H$
τ_y	yield stress

Subscripts

crit	critical
eff	effective
init	initial
m	ambient fluid
met	metamorphic aureole
(n)	function of n
S	function of S
sol	solid or solidus when used with temperature
sph	sphere

Acknowledgments. We would like to acknowledge our indebtedness to Harro Schmeling, who designed the computer code used to calculate the ascent velocity of cylinders through power law crust, and also to thank him for his continual support in the running of the program necessary to complete this work. We would also like to thank Harro Schmeling, Christopher Talbot, and Anders Wikström for inspiring discussion and ideas. The assistance of Sharon Ford for language editing and Christina Wernström for the figures is gratefully acknowledged.

References

- Astarita, G., and G. Apuzzo, Motion of bubbles in non-Newtonian liquids, *AIChE J.*, **11**, 815-820, 1965.
- Batchelor, G. K., *An Introduction to Fluid Dynamics*, 615 pp., Cambridge University Press, Cambridge, 1967.
- Bateman, R., On the role of diapirism in the segregation, ascent and final emplacement of granitoid magmas, *Tectonophysics*, **110**, 211-231, 1984.
- Berger, A. R., and W. S. Pitcher, Structures in granitic rocks: A commentary and critique on granite tectonics, *Proc. Geol. Assoc.*, **81**, 441-461, 1970.
- Beris, A. N., J. A. Tsamopoulos, R. C. Armstrong, and R. A. Brown, Creeping motion of a sphere through a Bingham plastic, *J. Fluid Mech.*, **158**, 219-244, 1985.
- Bhavaraju, S. M., R. A. Mashelkar, and H. W. Blanch, Bubble motion and mass transfer in Non-Newtonian fluids, I, Single bubble in power law and Bingham fluids, *AIChE J.*, **24**, 1063-1070, 1978a.
- Bhavaraju, S. M., R. A. Mashelkar, and H. W. Blanch, Bubble motion and mass transfer in Non-Newtonian fluids, II, Swarm of bubbles in a power-law fluid, *AIChE J.*, **24**, 1070-1076, 1978b.
- Biot, M. A., and H. Odé, Theory of gravity instability with variable overburden and compaction, *Geophysics*, **30**, 213-227, 1965.
- Byerlee, J., Friction of rocks, *Pure Appl. Geophys.*, **116**, 615-626, 1978.
- Chhabra, R. P., Hydrodynamics of bubbles and drops in rheologically complex liquids, In *Encyclopedia of Fluid Mechanics*, edited by N. P. Chermisinoff, pp. 253-286, Gulf, Houston, Tex., 1988.
- Clemens, J. D., and C. K. Mawer, Granitic magma transport by fracture propagation, *Tectonophysics*, **204**, 339-360, 1992.
- Crochet, M. J., A. R. Davies, and K. Walters, *Numerical Simulation of Non-Newtonian Flow*, Rheol. Ser., Vol. 1, 352 pp., Elsevier, New York, 1984.
- Cruden, A. R., Deformation around a rising diapir modeled by creeping flow past a sphere, *Tectonics*, **7**, 1091-1101, 1988.
- Cruden, A. R., Flow and fabric development during the diapiric rise of magma, *J. Geol.*, **98**, 681-698, 1990.
- Daly, S. F., and A. Raefsky, On the penetration of a hot diapir through a strongly temperature-dependent viscosity medium, *Geophys. J. R. Astron. Soc.*, **83**, 657-681, 1985.
- Dazhi, G., and R. I. Tanner, The drag on a sphere in a power-law fluid, *J. Non Newtonian Fluid Mech.*, **17**, 1-12, 1985.
- England, P., The genesis, ascent, and emplacement of the Northern Arran Granite, Scotland: Implications for granitic diapirism, *Geol. Soc. Am. Bull.*, **104**, 606-614, 1992.
- Grout, F. F., *Petrography and Petrology*, 522 pp., McGraw Hill, New York, 1932.
- Hadamard, J., Mouvement permanent lent d'une sphere liquide et visqueuse dans un liquide visqueux, *C. R. Acad. Sci.*, **152**, 1735-1738, 1911.
- Hansen, F. D., and N. L. Carter, Creep of selected crustal rocks at a 1000 MPa, *EOS, Trans. AGU*, **63**, 437, 1982.
- Happel, J., and H. Brenner, *Low Reynolds Number Hydrodynamics*, 553 pp., Martinus Nijhoff, Dordrecht, Netherlands, 1986.
- Hirose, T., and M. Moo-Young, Bubble drag and mass transfer in Non-Newtonian fluids creeping flow with power-law fluids, *Can. J. Chem. Eng.*, **47**, 265-267, 1969.
- Huppert, H. E., and S. J. Sparks, The generation of granitic melts by intrusion of basalt into continental crust, *J. Petrol.*, **29**, 599-624, 1988.
- Kawase, Y., and M. Moo-Young, Approximate solutions for power-law fluid flow past a particle at low Reynolds number, *J. Non Newtonian Fluid Mech.*, **21**, 167-177, 1986.
- Kerr, R. C., and J. R. Lister, Island arc and mid-ocean ridge volcanism, modelled by diapirism from linear source region, *Earth Planet. Sci. Lett.*, **88**, 143-152, 1988.
- Kirby, S. H., Rheology of the lithosphere, *Rev. Geophys.*, **21**, 1458-1487, 1983.
- Kukowski, H., and H. J. Neugebauer, On the ascent and emplacement of granitoid magma bodies. Dynamic-thermal numerical models, *Geol. Rundsch.*, **79**, 227-239, 1990.
- Levich, V. G., *Physicochemical Hydrodynamics*, 404 pp., Prentice-Hall, Englewood Cliffs, N.J., 1962.
- Lister, J. R., and R. C. Kerr, The effect of geometry on the gravitational instability of a buoyant region of viscous fluid, *J. Fluid Mech.*, **202**, 577-594, 1989.
- Mahon, K. I., T. M. Harrison, and D. A. Drew, Ascent of a granitoid diapir in a temperature varying medium, *J. Geophys. Res.*, **93**, 1174-1188, 1988.
- Marsh, B. D., Island arc development: Some observations, experiments and speculations, *J. Geol.*, **87**, 687-713, 1979.
- Marsh, B. D., On the mechanics of igneous diapirism, stopping, and zone melting, *Am. J. Sci.*, **282**, 808-855, 1982.

- Marsh, B. D., and L. H. Kantha, On the heat and mass transfer from an ascending magma, *Earth Planet. Sci. Lett.*, **39**, 435-443, 1978.
- McBirney, A. R., and T. Murase, Rheological properties of magmas, *Annu. Rev. Earth Planet. Sci.*, **12**, 337-357, 1984.
- Mhatre, M. V., and R. C. Kintner, Fall of liquid drops through pseudoplastic liquids, *Ind. Eng. Chem.*, **51**, 865-867, 1959.
- Miller, C. F., M. E. Watson, and T. M. Harrison, Perspective on the source, segregation and transport of granitoid magmas, *Trans. R. Soc. Edinburgh, Earth Sci.*, **79**, 135-156, 1988.
- Morris, S., The effects of a strongly temperature-dependent viscosity on slow flow past a hot sphere, *J. Fluid Mech.*, **124**, 1-26, 1982.
- Nakano, Y., and C. Tien, Creeping flow of power-law fluid over Newtonian fluid sphere, *AIChE J.*, **14**, 145-151, 1968.
- Paterson, M. S., Problems in the extrapolation of laboratory rheological data, *Tectonophysics*, **133**, 33-43, 1987.
- Paterson, S. R., R. H. Vernon, and T. K. Fowler, Aureole tectonics, in *Reviews in Mineralogy*, Vol. 26, edited by D. M. Kerrick, pp. 673-722, Book Crafters, 1991.
- Polyakov, A., and J. Podladchikov, Influence of the topography on the dynamics of the diapiric growth, *Geol. Soc. Am., Abstr. Programs*, A142, 1990.
- Ramberg, H., Model studies in relation to plutonic bodies, in *Mechanism of igneous intrusion*, edited by A. Newall and N. Rast, *Geol. J. Spec. Issue*, 261-286, 1970.
- Ramberg, H., *Gravity, Deformation and the Earth's Crust in Theory, Experiments and Geological Application* 2nd ed., 452 pp., Academic, London, 1981.
- Ribe, N., Diapirism in the earth's mantle: Experiments on the motion of a hot sphere in a fluid with temperature dependent viscosity, *J. Volcanol. Geotherm. Res.*, **16**, 221-245, 1983.
- Rönnlund, P., Viscosity ratio estimates from Rayleigh-Taylor instabilities, *Terra Nova*, **1**, 344-348, 1989.
- Rubin, A. M., Very viscous dikes in ductile rocks, *Earth Planet. Sci. Lett.*, in press, 1993.
- Rybczynski, W., Über die fortschreitende Bewegung einer flüssigen Kugel in einen zähen Medium, *Bull. Acad. Sci. Cracovie*, **1**, 40-46, 1911.
- Schmeling, H., A. R. Cruden, and G. Marquart, Finite deformation in and around a fluid sphere moving through a viscous medium: Implications for diapiric ascent, *Tectonophysics*, **149**, 17-34, 1988.
- Soula, J. C., Characteristics and mode of emplacement of gneiss domes and plutonic domes in central-eastern Pyrenees, *J. Struct. Geol.*, **4**, 313-342, 1982.
- Spera, F. J., A. Borgia, and J. Strimple, Rheology of melts and magmatic suspensions, 1, Design and calibration of concentric viscometer with application to rhyolitic magma, *J. Geophys. Res.*, **93**, 10273-10294, 1988.
- Turcotte, D. L., and G. Schubert, *Geodynamics: Application of Continuum Physics to Geological Problems*, 450 pp., John Wiley, New York, 1982.
- Weinberg, R. F., Internal circulation in a buoyant two-fluid Newtonian sphere: Implications for composed magmatic diapirs, *Earth Planet. Sci. Lett.*, **110**, 77-94, 1992.
- Weinberg, R. F., The upward transport of inclusions in Newtonian and power-law salt diapirs, *Tectonophysics*, **228**, 1-10, 1993.
- Weinberg, R. F., and H. Schmeling, Polydiapirs: Multiwavelength gravity structures, *J. Struct. Geol.*, **14**, 425-436, 1992.
- Whitehead, J. A., and D. S. Luther, Dynamics of laboratory diapirs and plume models, *J. Geophys. Res.*, **80**, 705-717, 1975.
- Wilks, K. R., and N. L. Carter, Rheology of some continental lower crustal rocks, *Tectonophysics*, **182**, 57-77, 1990.

Y. Podladchikov, Faculteit der Aardwetenschappen, Vrije Universiteit, De Boelelaan 1085, Amsterdam, Netherlands.

R.F. Weinberg, Research School of Earth Sciences, Australian National University, Acton, ACT 2601, Canberra, Australia.

(Received January 27, 1993; revised December 1, 1993; accepted December 6, 1993.)